Biosensors and Bioelectronics 129 (2019) 277–283

Contents lists available at ScienceDirect

Biosensors and Bioelectronics

journal homepage: www.elsevier.com/locate/bios

# Bisintercalating DNA redox reporters for real-time electrochemical qLAMP

Bo-Jun Chen[a], Veerappan Mani[a,b], Sheng-Tung Huang[a,b,*], Yi-Chiuen Hu[c], His-Chi Peter Shan[d]

[a] Department of Chemical Engineering and Biotechnology, National Taipei University of Technology, Taipei, Taiwan, ROC
[b] Graduate Institute of Biomedical and Biochemical Engineering, National Taipei University of Technology, Taipei, Taiwan, ROC
[c] National Applied Research Lab, Hsinchu, Taiwan, ROC
[d] WinSense Biotech Corporation, Hsinchu, Taiwan, ROC

ARTICLE INFO

*Keywords:*
DNA intercalating redox reporters
Real-time electrochemical qLAMP
Lab-on-chip
Automated gene detection devices
Single copy detection
POC applications

ABSTRACT

The electrochemical detection methods have emerged as a potential alternative to the bench-top optical systems in monitoring nucleic acid amplification. DNA intercalating redox reporters play a crucial role in such monitoring schemes. Here, a series of bisintercalating redox probes have been tailor-made to meet specific requirements of electrochemical quantitative loop-mediated isothermal amplification (qLAMP). The probes composed of two naphthoquinone-imidazole (NQIM) derivatives as signal motifs that are covalently bridged by different linkers (R). They are bis-NQIM-R; R = Alkane (Ak), ethylene glycol (EG) and phenyl (Ph). The linkers allow the probes to be fine-tuned for securing ideal redox reporter. DNA binding studies via electrochemical and fluorescence techniques demonstrate that the bis-NQIM-R probes possess better ds-DNA bisintercalating ability compared to their mono-analogs. The bis-NQIM-Ph was implemented in a real-time electrochemical qLAMP, for which a prototype custom-made device that can perform fully automated multiplexed analyses is devised. A single copy of *Salmonella* DNA was quantified in just 10 min and the performance is comparable to the benchtop fluorescence method. Thus, the bisintercalating redox reporters incorporated electrochemical detection schemes hold great promise in qLAMP.

## 1. Introduction

The development of portable, miniaturized, inexpensive, and robust gene detection devices at point-of-care (POC) has become increasingly important for on-site analyses in resource-limited areas (Martin et al., 2016a). The common gene detection approach involves the amplification of a target genetic sequence coupled with signal detection step (Petralia and Conoci, 2017). Irrespective of the type of amplification methods, signal revealing mechanism in all current instruments is depending on optical detection tools (Defever et al., 2011). However, optical equipments are delicate, bulky, fragile, expensive, and their extension of POC is limited (Defever et al., 2011). In addition, they are not suitable to analyze turbid or non-transparent biological samples and encountering restrictions over instrument miniaturization. In contrary, electrochemical instrumentations are simple, low-cost, portable, robust, low-power consuming, directly translates the analytical event into a digital signal, and desired for miniaturization and integration (Martin et al., 2016a). Besides, electroanalytical techniques are rapid, sensitive, and allowing analysis of non-transparent samples (Defever et al., 2009). Thus, the replacement of optical tools by electrochemical instruments is predicted to be a promising route for the POC appliances (Martin et al., 2016a). Specifically, electrochemical detection schemes coupled with loop mediated isothermal amplification (LAMP) has appeared to be the perfect combination (Ahmed et al., 2009), due to the compelling advantages of LAMP over traditional polymerase chain reaction (PCR) (Table S1) (Asiello and Baeumner, 2011; Qi et al., 2018).

In this direction, two types of electrochemical detection strategies are recommended based on the nature of the binding interaction between redox reporters and LAMP amplicons; electrostatic or intercalation (Ahmed et al., 2013; Patterson et al., 2013). So far, the intercalating redox reporters assisted route, which measures the consumption of reporters to track amplicons, appears to be promising (Martin et al., 2016b). In such case, the double-stranded DNA (ds-DNA) intercalating ability of the probe plays a pivotal role. Thus, the design of the ideal probes having optimal ds-DNA intercalating property and thermal stability are essential. The performances of various DNA intercalating substrates in the electrochemical quantitative LAMP (qLAMP) have been reviewed recently (Martin et al., 2016a). Hitherto, only three redox intercalating reporters are found applicable: osmium bipyridine-based complexes ($[Os(bpy)_2dppz]^{2+}$) (Defever et al., 2011), methylene blue (MB) (Hsieh et al., 2012; Luo et al., 2014), and methylene blue derivative (Martin et al., 2016b); yet, some of them holds

* Corresponding author at: Department of Chemical Engineering and Biotechnology, National Taipei University of Technology, Taipei, Taiwan, ROC.
*E-mail address:* ws75624@ntut.edu.tw (S.-T. Huang).

https://doi.org/10.1016/j.bios.2018.09.056
Received 1 July 2018; Received in revised form 30 August 2018; Accepted 16 September 2018
Available online 17 September 2018
0956-5663/ 

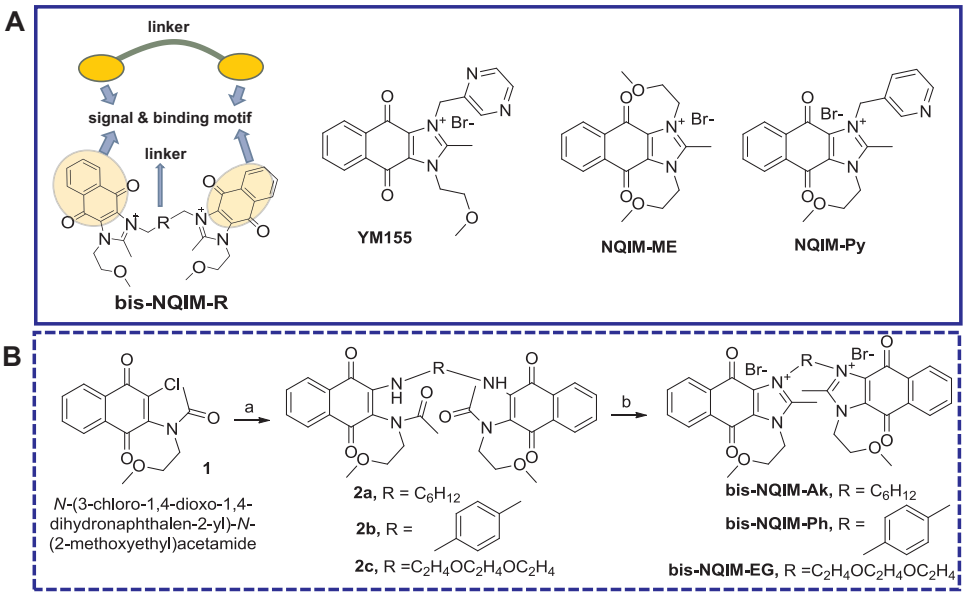


**Scheme 1.** (A) Design and chemical structures of bis-NQIM-R probes (R = Ak, Ph, and EG), YM155, mono-NQIM probes (NQIM-ME, NQIM-Py), and (B) The synthetic scheme to prepare bis-NQIM-R probes: The reagents and conditions: (a) $NH_2$-R-$NH_2$, toluene, $Et_3N$, 40 °C, 16 h, 60–70% yield; (b) 48% $HBr_{(aq)}$, ethanol/ethyl acetate 1:1 v/v, 55 °C, 16 h, 60–90% yield.

limitations. For instance, $[Os(bpy)_2dppz]^{2+}$ inhibits the polymerase activity at high concentrations, gives significant background drift and affects reproducibility. In addition, Os complexes are toxic and expensive. Notably, the existing reporters are not specially made for the exact needs of real-time qLAMP; but, they are just adopted from the commonly available list of electrochemical mediators.

Herein, a series of bisintercalating redox probes based on naphthoquinone-imidazole (NQIM) units (bis-NQIM-R; R = Alkane (Ak), phenyl (Ph), ethylene glycol (EG)) have been tailored to meet specific requirements of electrochemical qLAMP (Scheme 1A). The molecular design of these reporters is inspired from the chemical structure of well-known anticancer agent sepantronium bromide (YM155), which is known for its strong DNA intercalating property (Ho et al., 2015). The NQIM moieties are known to undergo a feasible two-electron redox process at the electrode surface. NQIM compounds are positively charged, water-soluble, possess salt structure, and able to attract phosphoric acid structure of DNA (Gómez et al., 2005; Palchaudhuri and Hergenrother, 2007). In fact, naphthoquinone derivatives are reported to be alternative redox mediator to osmium and ferrocene-based redox compounds in bioelectrocatalysis (Milton et al., 2015; Hasan et al., 2017). Probes with two intramolecular binding moieties are found to exhibit enhanced ds-DNA intercalating ability compared to their mono-analogs (Wilson et al., 2008). However, such probes have never been explored in electrochemical qLAMP. Moreover, the binding affinity of bis-analogs can be further tuned by suitably choosing the linkers, that are bridging binding motifs (Saeed et al., 2017). For this purpose, two linkers with a high number of possible molecular configurations (Ak and EG) and one linker with a lesser number of molecular configurations (Ph) are installed into the molecular backbone of probes. Accordingly, when the first NQIM moiety intercalates into ds-DNA, it facilitates the second NQIM moiety into DNA helix leading bisintercalation; thereby, allowing the formation of crescent-shaped complex.

Scheme 2 displays the general illustration of bis-NQIM-R bisintercalating probes coupled electrochemical qLAMP. Prior to LAMP process, bis-NQIM probes reveal larger electrochemical signals, because all the probe molecules are ionized freely in solutions and available for electrocatalysis. As the LAMP progresses, ds-DNA amplicons are exponentially produced in solutions. The as-produced amplicons bind with probes forming electrochemically inactive probe–DNA complex, as a result, the solution is depleted of free probes. Consequently, the remaining free bis-NQIM probes are lesser in amount, which reports a decreased signal on the voltammogram.

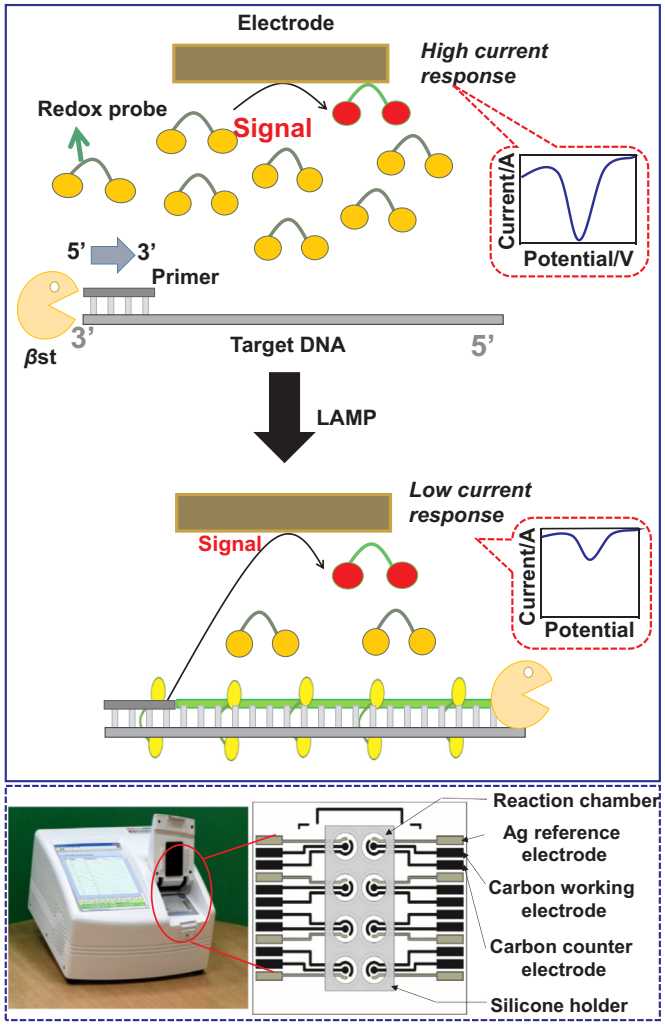


**Scheme 2.** (top) Schematic illustration of electrochemical qLAMP process of bisintercalating probes. (Bottom) Prototype homemade qLAMP device developed in our lab.

The development of automated electrochemical gene detection devices equivalent to that of gold-standard optical devices is still at

infancy; to date, only one real-time device that can work at automated closed-tube setup is reported (Martin et al., 2016b). Using bisintercalating probes as redox reporters for the first time, we described a rapid and sensitive electrochemical qLAMP for detecting a single copy of gene.

## 2. Experimental

### 2.1. Reagents

Electrochemical qLAMP was demonstrated by detecting the invasion gene (*invA*; GenBank accession number M90846) of *Salmonella enterica*, which was obtained from Dr. Chih-Hung Huang, National Taipei University of Technology, Taiwan. The primer sequences (FIP, BIP, F3, B3, Loop F, and Loop B for *Salmonella*) were used to specifically amplify the target genes. A set of six primers (given in Supporting information), namely, two outer (F3 and B3), two inner (FIP and BIP), and loop (Loop F; Loop F and Loop B), that can recognize eight distinct regions of target sequence was synthesized according to the previous literature methods (Chen et al., 2011). Deoxynucleotide (dNTP) solution, 10X isothermal amplification buffer, and *Bst* 3.0 DNA polymerase have been purchased from New England Biolabs Inc (NEB). Deoxyribonucleic acid sodium salt from calf thymus was purchased from Sigma-Aldrich. The chemicals and solvents were either puriss p.a. or purified by standard techniques. The reactions requiring anhydrous conditions were performed in oven-dried glassware under an Ar or a $N_2$ atmosphere. The stock solutions of probes are prepared in water.

The details of all the other chemicals, instrumentation, additional experimental details of electrochemical and fluorescence studies, schematic for experimental, detailed synthetical procedures, and characterizations are given in Supporting information. All the experiments were in triplicate, an average of three data was used to plot the figures.

### 2.2. Electrochemical studies

For binding studies, the electrochemical experiments were performed in a conventional three-electrode cell using glassy carbon electrode (GCE) as a working electrode (area = 0.070 $cm^2$), saturated Ag/AgCl (saturated KCl) as a reference electrode and Pt wire as a counter electrode. Prior to use, GCE was polished with 0.05 μm alumina and washed with double distilled (DD) water. Prior to electrochemical analysis, the electrolytes were deoxygenated with $N_2$ for 5 min. The optimized differential pulse voltammetry (DPV) parameters are amplitude = 0.05 V, pulse width = 0.05 s, sampling width = 0.0167 s and pulse period 0.5 s.

### 2.3. Real-time electrochemical tracking of qLAMP

LAMP was carried out in a reaction mixture (total volume of 25 μL) containing mixture of 2.5 μL target DNA (at concentrations ranging from $10^4$ to 1 copy/mL), 0.5 μL of each primer, 3 μL of deoxynucleotide (dNTP) solution mixture (1.2 mM), 1.5 μL probe (1 μM), 1.5 μL $MgSO_4$ (6 mM), 2.5 μL LAMP buffer (1 ×), 1 μL *Bst* 3.0 DNA polymerase (0.32 units/μL) and 10 μL of DD water (Table S2). The LAMP reaction was carried out in three steps: pre-treatment (40 °C, 5 min), LAMP reaction (65 °C, 30 min), and inactivation (80 °C, 3 min). The electrochemical signals were measured every 2 min in DPV mode. Background subtracted normalized current was used to make plots unless other specified.

### 2.4. Robust, portable, automated electrochemical qLAMP device

With assistance from the Winsense Company and the Instrument Technology Research Center (ITRI), Taiwan, we have developed a user-friendly, miniaturized, and portable eight-channel electrochemical qLAMP device that can perform rapid and accurate gene analyses at POC (Fig. S1). Both amplification (thermal controller module) and electrochemical equipments are integrated and automated. The device can monitor up to eight reactions in parallel. The instrumentation and working principle are given in Supporting information.

## 3. Results and discussions

### 3.1. Probes synthesis

The naphthoquinone-imidazole based mono-intercalating probes (NQIM-ME and NQIM-Py; ME = methyl ether and Py = pyridyl) were prepared in accordance with the published procedure (Ho et al., 2015). The synthetic scheme to prepare bis-NQIM-R is given in Scheme 1B. The preparation began with nucleophilic displacement of chlorine in known **1** (Ho et al., 2015) with 0.5 equivalent of the corresponding diamine to give dimer compounds **2a–c** in 60–70% yield. The final ring closure was performed by hydrobromic acid to give final compounds, bis-NQIM-R in 60–90% yield. The overall yield of two steps reaction is 36–63% from **1**. The chemical structures of synthetic intermediates and final products had been determined by $^1$H NMR, $^{13}$C NMR, FT-IR and ESI-mass, and the detail spectral results are attached in Supporting information.

### 3.2. Electrochemical properties of NQIM redox probes

The cyclic voltammetric (CV) behavior of bis- and mono-NQIM probes were tested in LAMP buffer at the scan rate of 50 mV $s^{-1}$ (Fig. S2A, B). The CVs are displayed a characteristic quasi-reversible redox couple that can be correlated to two electrons and two protons coupled naphthoquinone/reduced naphthoquinone reversible reactions (Gómez et al., 2005). The corresponding electrochemical parameters, anodic peak potential ($E_{pa}$), cathodic peak potential ($E_{pc}$), peak-to-peak separation ($\Delta E_p$), half-wave potential ($E_{1/2}$), anodic peak current ($I_{pa}$), cathodic peak current ($I_{pc}$), and ratio of $I_{pa}$ and $I_{pc}$ are listed in Table S3. The nature of different linkers had no effect on $E_{1/2.}$ The enhanced peak currents and minimized $\Delta E_p$ values are observed in the voltammograms of bisintercalators compared to that of monointercalators, indicating faster electron transfer of bisintercalators. In order to investigate the kinetics of bis-NQIM compounds, their voltammograms at different scan rates were recorded (Fig. S3). As the scan rate increases, the redox peak currents are linearly increased, while the peak potentials are shifted to higher potentials. The plots between redox peak currents and square root of scan rate displayed good linearity, indicating diffusion-controlled electrocatalysis of NQIM probes (insets to Fig. S3). Generally, osmium complexes are known for their faster kinetics on electrode surface compared to naphthoquinones. But, the novel design of probes (two reporting units in one molecule) might facilitate convincing electrode kinetics for bis-NQIM probes.

### 3.3. DNA binding studies

Next, the ds-DNA intercalating abilities of mono- and bis-NQIM redox substrates have been tested by monitoring their voltammograms in the presence (blue) and absence (red) of 100 μM calf thymus DNA in LAMP buffer (Fig. 1A-E). For all bis-NQIM probes, a significant drop in redox peak currents, alteration in current ratios, and positive shifts in peak potentials and $E_{1/2}$ were observed in presence of DNA. These voltammetric changes are primary evidence for the formation of probe-DNA complex. As described in the introduction section, the redox reporting unit (i.e., NQIM) of the probe is likely bounded (locked) into the double helix structure of DNA to form an electrochemically inactive probe-DNA complex, the resulting depletion of free-probes in solution causes the peak currents to decrease. The linear planar structure of bis-NQIM-R coupled with linker assistance is expected to stimulate bis-intercalation. Moreover, the probes are positively charged and own π electrons; therefore, fractional contributions from electrostatic, hydrogen bonding and π stacking interactions are also expected. The

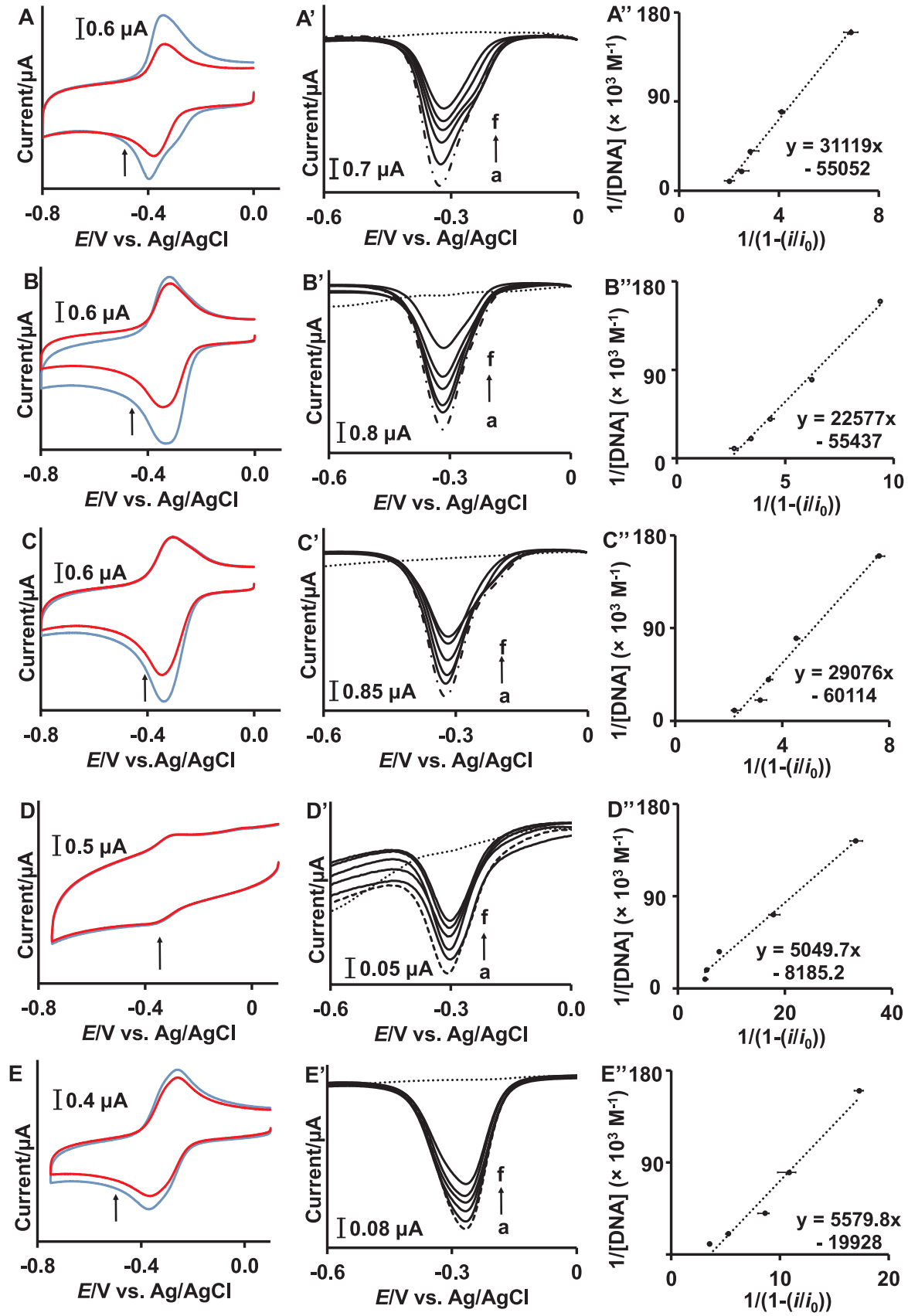


**Fig. 1.** CVs obtained for 5 μM bis-NQIM-EG (A), bis-NQIM-Ak (B), bis-NQIM-Ph (C), NQIM-ME (D), and NQIM-Py (E) in absence (blue) and presence (red) of 100 μM calf thymus DNA; scan rate = 50 mV $s^{-1}$. DPVs of 5 μM bis-NQIM-EG (A′), bis-NQIM-Ak (B′), bis-NQIM-Ph (C′), NQIM-ME (D′), and NQIM-Py (E′) in absence (a) and presence of 6.25 (b), 12.5 (c), 25 (d), 50 (e), and 100 μM (f) DNA and corresponding plots of $1/(1\text{-}i/i_0)$ vs. 1/[DNA] (A″ to E″). (For interpretation of the references to color in this figure legend, the reader is referred to the web version of this article.).

**Table 1**
DNA intercalating parameters of mono- and bis-NQIM probes; $K_b$ = binding constant, $s$ = binding site size, $D_f$ = diffusion coefficient of free probes and $D_b$ = diffusion coefficient of bound probes (presence of 100 μM calf thymus DNA) and bp = base pairs.

| Category | Probes | $K_b$ ($M^{-1}$) | $s$ (bp) | $D_f$ ($cm^2\ s^{-1}$) × $10^{-12}$ | $D_b$ ($cm^2\ s^{-1}$) × $10^{-12}$ |
|---|---|---|---|---|---|
| Mono-NQIM | NQIM-ME | 0.819 × $10^4$ | 1 | 13.74 | 9.556 |
| | NQIM-Py | 1.993 × $10^4$ | 6 | 2.279 | 1.101 |
| bis-NQIM | bis-NQIM-EG | 5.505 × $10^4$ | 4 | 9.282 | 2.736 |
| | bis-NQIM-Ak | 5.544 × $10^4$ | 4 | 12.49 | 8.624 |
| | bis-NQIM-Ph | 6.011 × $10^4$ | 4 | 17.82 | 8.144 |

mono-probes show poor DNA binding capacity compared to their bis analogs, as evident from minimal decreases in redox currents upon DNA binding (Fig. 1D, E). Possibly, a single unit of NQIM is not sufficient to facilitate strong intercalation.

### 3.4. Binding parameters

Next, the DNA-binding characteristic of NQIM probes was further analyzed by DPV. The DPV currents follow a decreasing trend, as the amount of incubated DNA increases, (Fig. 1A′-E′). The mono-analogs displayed poor intercalating ability compared to their bis-analogs, consistent with CV results. Their binding constants ($K_b$) have been calculated from the plot of $1/(1–i/i_0)$ vs. 1/[DNA] (Fig. 1A″-E″) and Eq. (1) [Shah et al. (2010)] and given in Table 1.

$$\frac{1}{[DNA]} = \frac{K_b\ (1-A)}{1-(i/i_0)} - K_b \quad (1)$$

Here, $K_b$ is binding constant, $i$ and $i_0$ are DPV currents of probes in presence and absence of DNA and $A$ is proportionality constant. The values of $K_b$ follow this trend: bis-NQIM-Ph > bis-NQIM-Ak > bis-NQIM-EG > NQIM-Py > NQIM-ME. The $K_b$ values of bis-NQIM probes are several folds higher than mono-analogs. For instance, the $K_b$ of bis-NQIM-Ph is 3.02 and 7.35 folds larger than NQIM-Py and NQIM-ME, respectively. Thus, the $K_b$ results authenticated that probes containing two units of NQIM had retained better DNA intercalating properties than that contain one such unit, which is consistent with previous reports as well (Wilson et al., 2008). Among bisintercalators, bis-NQIM-Ph possesses better $K_b$, which might be due to the effect of linkers. The $K_b$ values of bis-NQIM probes are either superior or comparable to the previous reports (Table S4). Although, our probes have lesser binding affinity compared to previously reported $[Os(bpy)_2dppz]^{2+}$; we still able to report novel bisintercalating redox mediators that are not depending on the use of toxic and expensive Os (Deféver et al., 2011).

Next, the binding sites size ($s$) (in base pairs) was calculated from the plot of [bound probes]/[free probes] ($C_b/C_f$) vs. [DNA] (Fig. S4) and Eq. (2),

$$\frac{C_b}{C_f} = \frac{i-i_0}{i} = \frac{K_b}{2s}[DNA] - K_b C_b \quad (2)$$

The obtained range of $s$ values (Table 1) is within the expected average size ranges of 1–20 base pairs (Arshad et al., 2012). The $s$ values slightly differ among mono- and bis- category. But, they were identical for all bisintercalators, suggesting the linkers have no influence on $s$.

The diffusion co-efficients ($D$) of NQIM redox reporters in absence and presence of calf thymus DNA were calculated from the plot of peak currents vs. $(\text{scan rate})^{1/2}$ (Fig. S5) and Randles–Sevcik equation ($i = 2.69 \times 10^5\ n^{3/2}\ A\ C_0^*\ D^{1/2}\ v^{1/2}$). Here, $n$ = number of electrons involved in rate-determining step, $v$ = scan rate ($V\ s^{-1}$) and $C_o^*$ = concentration of probes. The $D$ values of bis-probes are significantly decreased after the probes bound to DNA (Table 1), thus added additional evidence for their DNA binding potential (Lin et al., 2016). Generally, the probes-DNA complex is larger in size compared to free probes causing decreased diffusion rate.

### 3.5. Fluorescence studies

Studies indicate the nature and strength of probe-DNA interaction have a significant influence on the analytical outcome of electrochemical qLAMP (Martin et al., 2016b). The nature of the interaction between NQIM probes and DNA was analyzed by monitoring their ability to replace ethidium bromide (EtBr) from EtBr-DNA complex. EtBr binds with DNA via intercalation and produces DNA-EtBr complex, which reveals an intense fluorescence at a wavelength of 625 nm in the emission spectrum (Fig. S6A-D) (Burmudžija et al., 2016). However, a considerable decrease in their signal intensity was observed in presence of NQIM probes. Moreover, the decrease was linear as the concentrations of NQIM probes increases. i.e., fluorescence quenching is observed in presence of NQIM probes. Possibly, there might be a competition between NQIM probes and EtBr in binding with DNA. Due to the superior intercalating ability of NQIM probes, they replace EtBr from EtBr-DNA complex. The replacement is possible only when NQIM probes are stronger than EtBr and binding via intercalation. The stronger the intercalation, the larger the quenching; as expectedly bisintercalating NQIM probes displayed better quenching effect on EtBr-DNA complex than mono-analogs (Fig. S6A-D). Thus, NQIM probes are strong binds with DNA via intercalation.

The fluorescence quenching of NQIM probes can be correlated by the Stern–Volmer equation; $I_0/I = 1 + k_q\ \tau_0\ [Q] = 1 + K_{SV}\ [Q]$. Here, $I_0$ and $I$ are fluorescence intensities in absence and presence of probes, [Q] is the concentration of quencher (i.e., NQIM probes), $k_q$ is quencher rate coefficient, and $\tau_0$ is lifetime of DNA without a quencher. $K_{sv}$ is Stern–Volmer quenching constant, which can be calculated from the slope of plot between $I_0/I$ and [probes] (Fig. S6E). The $K_{sv}$ values are ascending in the following order: NQIM-Py ($1.25 \times 10^3\ M^{-1}$) < bis-NQIM-EG ($1.35 \times 10^4\ M^{-1}$) < bis-NQIM-Ak ($1.42 \times 10^4\ M^{-1}$) < bis-NQIM-Ph ($3.01 \times 10^4\ M^{-1}$). The bis-NQIM-EG, bis-NQIM-Ak, and bis-NQIM-Ph are exhibiting 10.8, 11.4 and 24.1 folds higher $K_{sv}$ than NQIM-Py, which confirms the enormous contribution of bisintercalation in binding. In addition, the $K_{sv}$ of bis-NQIM-Ph is either comparable or superior to the previously reported probes, such as MB ($7.60 \times 10^3\ M^{-1}$) (Hajian et al., 2009) and ferrocene derivative ($2.5 \times 10^4\ M^{-1}$) (Burmudžija et al., 2016).

At the same time, the $K_{sv}$ values are slightly differed based on the types of linker chains. It is known that when the linker chain rotations are restricted, the numbers of molecular confirmations of the compound in solutions are reduced and this kind of effects is observed in trimethyl lock effect (Huang and Lin, 2006). We presume similar kinds of effect is operating in the bis-NQIM probes, which likely affects the intercalating capacity of probes.

For instance, the linkers installed in bis-NQIM-Ak and bis-NQIM-EG are mostly single bonds and they are freely rotated in solutions, which are resulting with large possible numbers of molecular configurations in solutions. In contrast, the linker placed in bis-NQIM-Ph is mostly unrotatable π bonds with limited number of rotatable single bonds; therefore, the number of molecular configurations are limited as compared to bis-NQIM-Ak and bis-NQIM-EG. When the first unit of NQIM in bis-NQIM-Ph is intercalated into DNA, the activity of its linker chain (i.e., Ph) is lowered by limited numbers of molecular configurations, which then facilitates the second unit of NQIM to intercalate with DNA and forms crescent-shaped complex (Fig. S7A). As a result, bis-NQIM-Ph deserved to hold supreme binding ability for the competitive replacement of EtBr in EtBr-DNA complex (Fig. S7B). Compared to Ph group, the abilities of EG and Ak linkers to facilitate the binding of second

NQIM moiety is inadequate, because of their higher numbers of molecular configurations. As a result, 2.23 and 2.12 folds lesser $K_{sv}$ values are observed for NQIM-EG and bis-NQIM-Ak compared to bis-NQIM-Ph, respectively. Accordingly, their competitive binding in EtBr-DNA complex is also affected.

### 3.6. Thermal stability and LAMP inhibitory studies

The redox reporter should able to withstand the amplification temperature in order to be used in LAMP reactions. To this purpose, two different concentrations of bis-NQIM probes (1 and 20 μM) were incubated in LAMP buffer, isothermally treated at 65 °C and corresponding DPVs are analyzed (Fig. S8). Under LAMP conditions, all bisintercalators are able to maintain more than 90% of their initial current response up to 40 min, demonstrating good thermal stability.

Generally, the strong DNA intercalating probes are able to furnish better analytical performance. But at the same time, probes should not bind too much to avoid inhibition of LAMP reaction (Martin et al., 2016a). The LAMP inhibition properties of bis-NQIM probes have been investigated by gel electrophoresis at their low (1 μM) and high (20 μM) concentrations (Fig. S9). Regardless of different concentrations, the brightness produced by LAMP products in absence of probes is identical to that in presence of probes, revealing that they are not disturbing LAMP process.

### 3.7. Rapid sensing of single gene copy

A thorough investigation on binding potentials of NQIM probes led us to conclude that bis-NQIM-Ph is the perfect redox reporter; hence, it was selected for electrochemical qLAMP. The *salmonella* SL1344 gene was chosen as a model target. The DPV currents obtained for different copy numbers of the target ($10^4$, $10^3$, $10^2$, $10^1$, 10° and negative control) was monitored up to 30 min in real-time. The normalized current response was plotted against time (Fig. 2A). A typical exponential signal decrease from a characteristic time-to-threshold ($t_t$) value was observed. For the high concentration of templates ($10^5$ copies), an earlier occurrence of onset-signal decrease was noticed. No drift in the background was observed, indicates baseline stability.

Then, the change in current derivative (dI/dt) was plotted against time to find $t_t$ (Fig. 2B). When the highest concentration of target is added, a rapid drop in the current derivative was observed within 6 min. A lower-level signal decline was observed for lower concentrations of the target; but, it can still be detected in 10–12 min when dropped to a single copy number. The negative control i.e., without template indicates no any significant changes in DPV and the corresponding plots are just baselines.

A standard calibration plot between $t_t$ and logarithmic input of target displayed good linearly (Fig. 2C) and the result is compared with routinely used MB probe incorporated in fluorescent qLAMP as well as electrochemical qLAMP. The reachable detection limits for all three methods are same, i.e., 1 copy number. However, the least $t_t$ of our method compared to bench-top methods indicates its standing merit in rapid sensing. For 1-copy detections, the $t_t$ values obtained for bis-NQIM-Ph, MB/fluorescence qLAMP and MB/electrochemical LAMP were of 10, 23, and 22 min; thus, just half of $t_t$ is required for bis-NQIM-Ph to detect single copy SL1344 per microliter. The $t_t$ value at bis-NQIM-Ph is also better than previously reported other probes (Table 2). Besides, our method requires fewer amounts of probe compared to previous reports. For instance, our method works well at 1 μM of bis-NQIM-Ph, however, MB incorporated assays require high concentrations. Moreover, our electrochemical qLAMP device has several advantageous; lighter (5–10 times), more portable (270 × 265 × 156 $mm^3$, 6 kg), in-built with multiple electrochemical techniques and possessed a user-friendly touch-screen control interface, and designed to be suitable and convenient for POC applications.

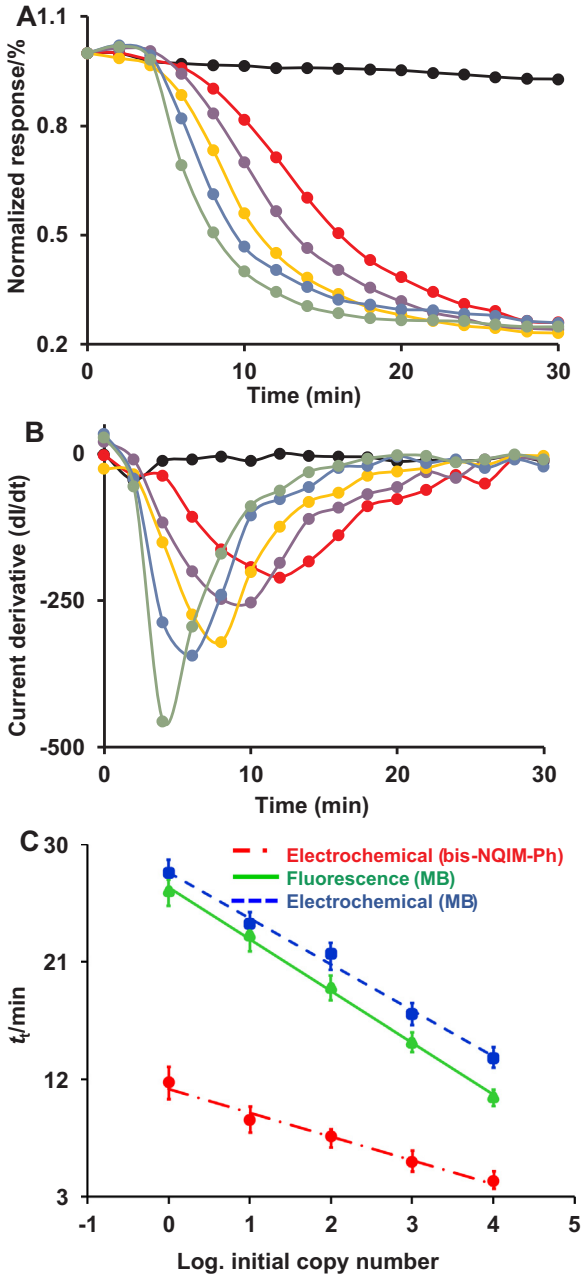


**Fig. 2.** (A) Time course amplification curve obtained from real-time electrochemical qLAMP with samples containing $10^4$ (green), $10^3$ (blue), $10^2$ (orange), $10^1$ (violet), 10° (red), and 0 (Negative control, black) copies of *Salmonella* SL1344. (B) Current derivative (dI/dt) vs. time (min.) (C) Standard calibration plots of $t_t$ vs logarithmic input of target: Fluorescent qLAMP using MB (green, solid line) and electrochemical qLAMP using MB (blue, dash line) and bis-NQIM-Ph (red, dash dot line). $t_t$ is defined as the reaction time required to reach sufficiently positive signals above the baseline. (For interpretation of the references to color in this figure legend, the reader is referred to the web version of this article.).

## 4. Conclusions

A series of tailor-made bisintercalating redox reporters have been synthesized and their ds-DNA binding abilities were explored. Bisintercalating probes possess superior ability compared to their mono-analogues. The major type of interaction between probes and DNA is intercalation. Although NQIM probes are showing poor binding affinity compared to existing $[Os(bpy)_2dppz]^{2+}$ complex; still, they are competent for qLAMP. Ideally, bis-NQIM-Ph exhibited superior ds-DNA

**Table 2**
Comparison of bis-NQIM-Ph coupled electrochemical qLAMP with previous reports.

| Method | Probe | LOD (copy/μL) | $t_t$ (min) | Ref. |
|---|---|---|---|---|
| Fluorescence | – | 1 | ~35 | (Fan et al., 2015) |
| Fluorescence | calcein | 1.057 | – | (Li et al., 2016) |
| Fluorescence | MB | 1 | ~23 | This work |
| Electrochemical | MB | 1 | ~22 | |
| Electrochemical | Bis-NQIM-Ph | 1 | ~10 | |

intercalating ability, withstood LAMP temperature condition, did not inhibit LAMP reactions, and affords rapid and ultrasensitive detection. A rapid and sensitive gene detection platform is established by employing bis-NQIM-Ph as a redox reporter; a single copy detection of SL1344 was achieved in just 10 min. The described electrochemical qLAMP device is smaller, lighter, more portable, inbuilt with multiple electroanalytical techniques, and easy-to-use. The future work will be directed to test its POC applications in field environments.

## Acknowledgements

This work was supported by the Ministry of Science and Technology, Taiwan (Republic of China) (MOST 106-2113-M-027-005, MOST 105-2119-M-027-001-CC3).

## Appendix A. Supplementary material

Supplementary data associated with this article can be found in the online version at doi:10.1016/j.bios.2018.09.056.

## References

Ahmed, M.U., Nahar, S., Safavieh, M., Zourob, M., 2013. Analyst 138, 907–915.
Ahmed, M.U., Saito, M., Hossain, M.M., Rao, S.R., Furui, S., Hino, A., Takamura, Y., Takagi, M., Tamiya, E., 2009. Analyst 134, 966–972.
Arshad, N., Yunus, U., Razzque, S., Khan, M., Saleem, S., Mirza, B., Rashid, N., 2012. Eur. J. Med. Chem. 47, 452–461.
Asiello, P.J., Baeumner, A.J., 2011. Lab Chip 11, 1420–1430.
Burmudžija, A., Ratković, Z., Muškinja, J., Janković, N., Ranković, B., Kosanić, M., Đorđević, S., 2016. RSC Adv. 6, 91420–91430.
Chen, S., Wang, F., Beaulieu, J.C., Stein, R.E., Ge, B., 2011. Appl. Environ. Microbiol. 77, 4008–4016.
Deféver, T., Druet, M., Evrard, D., Marchal, D., Limoges, B., 2011. Anal. Chem. 83, 1815–1821.
Deféver, T., Druet, M., Rochelet-Dequaire, M., Joannes, M., Grossiord, C., Limoges, B., Marchal, D., 2009. J. Am. Chem. Soc. 131, 11433–11441.
Fan, F., Du, P., Kan, B., Yan, M., 2015. PLoS One 10, 1–13.
Gómez, M., González, F.J., González, I., 2005. J. Electroanal. Chem. 578, 193–202.
Hajian, R., Shams, N., Mohagheghian, M., 2009. J. Braz. Chem. Soc. 20, 1399–1405.
Hasan, K., Grattieri, M., Wang, T., Milton, R.S., Minteer, S.D., 2017. ACS Energy Lett. 2, 1947–1951.
Ho, S.-H.S., Sim, M.-Y., Yee, W.-L.S., Yang, T., Yuen, S.-P.J., Go, M.-L., 2015. Eur. J. Med. Chem. 104, 42–56.
Hsieh, K., Patterson, A.S., Ferguson, B.S., Plaxco, K.W., Soh, H.T., 2012. Angew. Chem. Int. Ed. 124, 4980–4984.
Huang, S.-T., Lin, Y.-L., 2006. Org. Lett. 8, 265–268.
Li, J., Zhai, L., Bie, X., Lu, Z., Kong, X., Yu, Q., Lv, F., Zhang, C., Zhao, H., 2016. Food Control 60, 230–236.
Lin, Y.-J., Wu, Y.-C., Mani, V., Huang, S.-T., Huang, C.-H., Hu, Y.-C., Shan, H.-C.P., 2016. Biosens. Bioelectron. 79, 294–299.
Luo, J., Fang, X., Ye, D., Li, H., Chen, H., Zhang, S., Kong, J., 2014. Biosens. Bioelectron. 60, 84–91.
Martin, A., Bouffier, L., Grant, K.B., Limoges, B., Marchal, D., 2016a. Analyst 141, 4196–4203.
Martin, A., Grant, K.B., Stressmann, F., Ghigo, J.-M., Marchal, D., Limoges, B., 2016b. ACS Sens. 1, 904–912.
Milton, R.S., Hickey, D.P., Abdellaoui, S., Lim, K., Wu, F., Tan, B., Minteer, S.D., 2015. Chem. Sci. 6, 4867–4875.
Palchaudhuri, R., Hergenrother, P.J., 2007. Curr. Opin. Biotechnol. 18, 497–503.
Patterson, A.S., Hsieh, K., Soh, H.T., Plaxco, K.W., 2013. Trends Biotechnol. 31, 704–712.
Petralia, S., Conoci, S., 2017. ACS Sens. 2, 876–891.
Qi, H., Yue, S., Bi, S., Ding, C., Song, W., 2018. Biosens. Bioelectron. 110, 207–217.
Saeed, H.K., Saeed, I.Q., Buurma, N.J., Thomas, J.A., 2017. Chem. Eur. J. 23, 5467–5477.
Shah, A., Zaheer, M., Qureshi, R., Akhter, Z., Nazar, M.F., 2010. Spectrochim. Acta. Part A 75, 1082–1087.
Wilson, B., Fernández, M.-J., Lorente, A., Grant, K.B., 2008. Org. Biomol. Chem. 6, 4026–4035.